


Review

Novel Materials for Heavy Metal Removal in Capacitive Deionization

Youze Xu ¹, Zhenyu Zhong ¹, Xianhui Zeng ², Yuanyuan Zhao ¹, Wenting Deng ² and Yuehui Chen ^{2,*} 

¹ Key Laboratory of Water Pollution Control Technology, Hunan Province, Hunan Research Academy of Environmental Sciences, Changsha 410004, China; youzexing@163.com (Y.X.)

² School of Environmental and Resources, Xiangtan University, Xiangtan 411105, China

* Correspondence: E-mail address: YHchen@xtu.edu.cn

Abstract: Heavy metals are considered a class of contaminant that can accumulate in the food chain and thus must be removed from contaminated media. Heavy metals can be removed by electrocoagulation, electroflotation, electrodialysis, capacitive deionization, and so on. Among the methods to remove heavy metals, capacitive deionization is one of the most attractive methods that can remove heavy metal ions without using a large volume of chemicals and producing a high number of heavy metals containing solid wastes. In this study, after a brief introduction to the mechanism of capacitive deionization, we focus on materials that have been developed as electrodes for heavy metal removal in capacitive deionization and summarize the latest advancements. Finally, with particular emphasis on material design, we provide some further insights in this area.

Keywords: capacitive deionization; heavy metal removal; electrode material; electrosorption



Citation: Xu, Y.; Zhong, Z.; Zeng, X.; Zhao, Y.; Deng, W.; Chen, Y. Novel Materials for Heavy Metal Removal in Capacitive Deionization. *Appl. Sci.* **2023**, *13*, 5635. <https://doi.org/10.3390/app13095635>

Academic Editors: Qingzhu Li, Weizhen Liu and Zhenhua Zhang

Received: 7 March 2023

Revised: 17 April 2023

Accepted: 20 April 2023

Published: 3 May 2023



Copyright: © 2023 by the authors. Licensee MDPI, Basel, Switzerland. This article is an open access article distributed under the terms and conditions of the Creative Commons Attribution (CC BY) license (<https://creativecommons.org/licenses/by/4.0/>).

1. Introduction

Industrialization brings about the rapid transformation of manufacturing and leads to higher productivity, raising living standards. However, this process also brings threats to human beings such as the pollution of air, water, and soil, which can result in significant deterioration of quality of life and life expectancy [1]. Heavy metals (HMs) are regarded as one of the most important categories of pollutants and have caused wide concern due to their high toxicity and bioaccumulative properties. The bioaccumulative process leads to the pollution of air, water, and soil and eventually leads to adverse effects on humans. HMs have no rigorous definition on a scientific and chemical basis [2]. Generally, HMs have a density of over 5 g cm^{-3} (5 times $> \text{H}_2\text{O}$), meaning a metal with a density below this lacks heavy metal chemistry. Thus, HM properties are partially related to density as well as their chemical properties; they contain transition and post-transition elements along with metalloids, namely arsenic and selenium. Moreover, HMs are regarded as “toxic elements” priority contaminants listed by the United States Environmental Protection Agency [3]. A large number of HMs, with the exceptions of Cd, Hg, and Pb, are also essential micronutrients for living organisms; they only become toxic when the concentration is over the limit [4,5]. The dosage that determines either HM toxicity or micronutrient properties is the critical criterion with which to identify the toxicity of HMs [6].

Sources of HMs can be natural such as landslides, weathering, and volcanic eruptions, but they mainly originate from anthropogenic processes such as mining, agriculture, electroplating fossil fuel combustion, and waste disposal. For instance, agricultural use of HMs in the form of pesticides and fertilizer as well as corrosion and industrialization releases HMs into the environment [7,8]. Untreated wastewater containing heavy metals discharged into the natural environment can pollute water bodies and soil, endangering food safety and human health through the food chain [8]. An increase in concern for public health has led to the enactment of varied legislation to control the emission of HMs [9]. This increase in public health concern has led to the enactment of varied HM emissions control

legislation. This leads to an eruption of interest in developing new technologies to control emissions. Widely applied technologies for HM removal are based on solid-phase extraction using precipitation, coagulation, and flocculation [10]. However, a major concern with this technology is its output of heavy metal solids, which become solid waste. Conversely, liquid-phase extraction based on new technologies such as adsorption, ion exchange, and membrane separation has gained much interest because these processes concentrate metal ions directly devoid of a huge amount of solid heavy metal-containing waste. However, new advanced liquid phase extraction methods are highly dependent on emerging new materials such as adsorbents and ion exchangers, membranes, and electrochemical adsorption materials. [11,12]. In the past several decades, great efforts have been made toward developing new materials for heavy metal removal. With the exception of adsorption and membrane filtration processes, electrochemical treatments for HM removal are gaining increasing interest. These methods use electrostatic fields to dry metal ions and enhance precipitation, adsorption, and separation. And this paper reviews the electrochemical treatment technology of heavy metal wastewater, which can provide a reference for the development of efficient and energy-saving heavy metal wastewater treatment technology. Figure 1 summarizes electrochemical methods for HM removal. These electrochemical methods can be classified into electrocoagulation, electroflotation, electrodialysis, and electrodeposition depending on their mechanism.

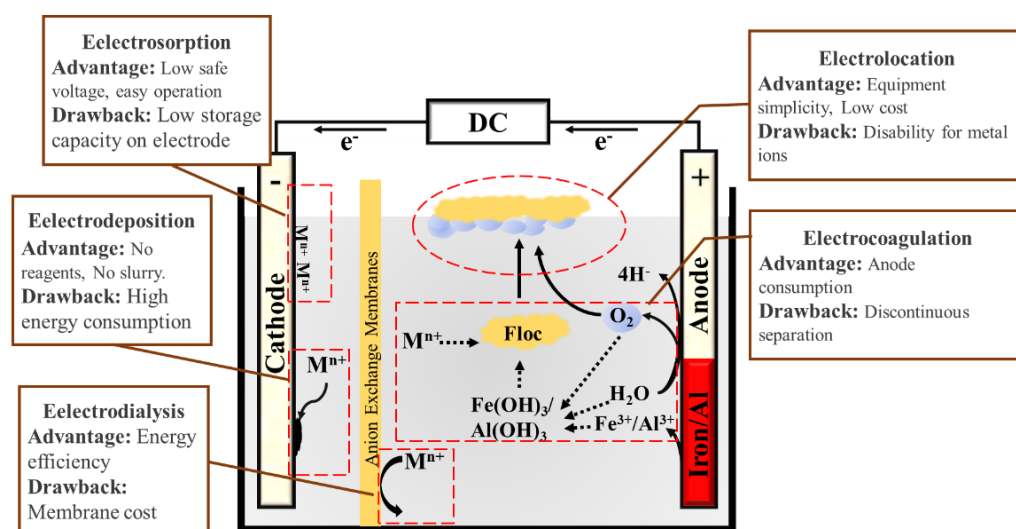


Figure 1. Electrochemical methods for heavy metal removal.

2. A Brief Review of Electrochemical Methods

Electrocoagulation (EC) is currently an efficient technology in wastewater treatment [13]. EC is a process involving the in situ generation of coagulants such as aluminum/iron ions and corresponding hydroxides from the electrical dissolution of “sacrificial anodes” under direct electrical currents [14]. Generated iron or aluminum flocs serve as coagulants and subsequently precipitate HMs, and an aluminum plate, steel/iron plate/mesh, and Ti plate/mesh are applied as anode and cathode materials to remove Cr(VI), Cu(II), Ni(II), Cd(II), Pb(II), Zn(II), Ba(II), and As(III) [15–23]. The EC process can dispose of multiple contaminants in one process; has low sludge production and maintenance costs; can easily handle water quality variations; and can achieve over 95% removal efficiency for HMs. [15,18,22]. The disadvantages of EC are as follows: (1) The dissolution of “sacrificial electrodes” into wastewater occurs due to oxidation, which requires frequent disposal. (2) The passivation of electrodes over time has limited its implementation. (3) The use of electricity may be expensive in many places. (4) High conductivity of the wastewater suspension is required [24–26].

Electroflotation (EF) is suitable for separating complex heavy metal wastewater with heterotic contaminants such as sludge. In this process, water is split into oxygen and hydrogen electrodes. Gas bubbles are generated, and the suspended contaminants are raised to the water surface. In this complicated process, bubble size and gas generation rate are two crucial factors in metal efficiency, deeply dependent on the current density used [27]. EF is gaining interest because its system produces a fine gas bubble without turbulence, the bubbles exhibit good coverage of the whole area, and the system is suitable for full automatization. The EF process has been applied in the food industry; oily wastewater; chemical wastewaters; effluents from the sugar and leather industries; and farms as well as in the dairy industry, and thus has been successfully commercialized [28]. Gas bubbles are the workhorse of EF, and bubble size is the key parameter for determining efficiency. Recently, a coupled method combining EF and EC to remove and separate heavy ions has been scaled up in industry [29]. In such a process, metal ions are coagulated and floated over the water surface [30]. The drawbacks of EF are the insufficiently high productivity of its units; the release of H₂ bubbles; the cost of electrodes and maintenance; and the formation of sludge by volume [31].

The EF system relies on hydrogen and oxygen/chloride produced at the cathode and anode, respectively, which are referred to as the hydrogen evolution reaction and oxygen/chloride evolution reaction, respectively. These processes are particularly energy-consuming due to the water-splitting process, requiring a potential over 1.5 V even when using the best-developed catalysts. Presently, the most widely applied anode materials in EF systems are stainless steel, nickel plates, titanium, and carbon cloths due to their cheap price and relatively good HER ability [32,33]. Anode materials should be chemically stable since the electrodes are working at high potentials (1–3 V). Iron, aluminum, and stainless steel are cheap but suffer from corrosion [34]. Graphite and other carbon-based materials are relatively stable but exhibit high overpotential for OER [35]. Dimensionally stable anodes (DSA) are the most attractive anodes for EF [36,37]. The electrodes are developed using conductive precious RuO₂, IrO₂, and their composite metal oxides as the electrocatalysts, normally using TiO₂, Nb₂O₅, Ta₂O₅, and ZrO₂ as the stabilizing agents supported on a Ti-, Ta-, W-, etc. -based metal substrate [37,38]. The major merits of these materials are their high stability and long lifetimes even in low-pH solution; thus, these anodes provide an attractive alternation for EF.

Electrodialysis (ED) is used to transport metal ions between two solutions along ion-exchange membranes under the influence of an applied electric potential difference. ED is an established technology in treating industrial wastewater; wastewater from the drug and food industries; table salt production; chemical processes; and HMs removal [22,39]. It is conducted in a configuration called an ED cell [40]. The ED process can purify water without phase change, reaction, or chemicals [41]. These merits provide environmental benefits without the use of fossil fuels or chemical detergents. However, ED technology has limitations, including scaling, membrane fouling, energy consumption, and selectivity [42,43]. ED has been investigated for the removal of Cr(VI) [44,45], Cu(II) [46], Zn(II) [47], Ni(II) [48], and Ag(I) [49]. ED systems necessitate excellent ion exchange membranes with lower electrical resistance, mechanical durability, improved permeability, and higher selectivity for specific ions. Production costs have also come under consideration [32], which is discussed in this paper's section on membranes.

Electrodeposition (EP) is a practical method that relies on the redox reduction of anodes alone. Heavy metal ions are reduced and deposited on an electrode in solid form. This process allows the simultaneous removal and recovery of HMs from wastewater [50,51]. High removal and recovery efficiency have been reported for the disposal of As(V)-, Cr(VI)-, and Cu(II)-containing wastewaters [51,52]. However, the reaction degree and side reactions such as water splitting were hard to control due to high energy dissipation [25]. Table 1 summarizes the application of EC, EF, and EP for heavy metal removal.

Table 1. Electrochemical methods for heavy metal removal.

Metal	Method	Cathode	Anode	Ref
Cr ⁶⁺	Reverse electrodialysis	Carbon felt	Ti/IrO ₂ -Ta ₂ O ₅	[44]
Cr ⁶⁺	Reverse electrodialysis	Carbon felt	Biotic anode	[45]
Cr ⁶⁺	Electrocoagulation	Cylindrical vessel iron cathode	Vertical rotating impeller Fe anode	[15]
Cr ⁶⁺	Electrocoagulation	Air cathode	Pure sacrificial iron plate	[16]
Cr ⁶⁺	Microbial fuel cell	Carbon brush	Carbon felt	[53]
Cr ⁶⁺				[54]
Cr ⁶⁺	Microbial fuel cell	Graphite rods	Polyaniline-modified carbon Fe	[55]
Cr ⁶⁺	Alkaline ethanol fuel cell	Carbon fiber cloth	Carbon-fiber-cloth-coated Pt	[56]
Pb ²⁺	Fuel cell	Carbon cloth	Carbon-cloth-coated Ni	[57]
Cr ⁶⁺	Solar electrocoagulation	Perforated Zn	Perforated Zn	[17]
Cu ²⁺ ; Cr ⁶⁺ ; Ni ²⁺ ;	Electrocoagulation–electroflotation	Stainless steel	Al	[58]
Cd ²⁺	Electrocoagulation	Zn	Zn	[18]
Pb ²⁺ ; Zn ²⁺ ; Cd ²⁺ ;	Electrocoagulation	Stainless steel	Al	[19]
As ³⁺	Electrocoagulation	Fe plate	Al plate	[20]
Cd ²⁺ ; Cu ²⁺	Electrocoagulation	Al plate	Al plate	[21]
Zn ²⁺	Electrocoagulation	Stainless steel plate	Ti expanded mesh	[59]
Cu ²⁺	Electro-Fenton method	Graphite	Fe	[32]
Cr ³⁺ ; Cu ²⁺ ; Ni ²⁺ ; Zn ²⁺	Electroflotation	Stainless steel	Ti plate	[60]
Fe ³⁺ ; Cu ²⁺ ; Zn ²⁺	Electrocoagulation	Iron (carbon steel) plates	Iron (carbon steel) plates	[61]
Cu ²⁺ ; Zn ²⁺ ; Ni ²⁺ ; Ag ⁺	Microbial fuel cell	Activated carbon	Carbon fiber veil	[49]
Ni ²⁺ ; Cu ²⁺	Microfluidic electrodialysis	Au	Au	[62]
Mo ⁴⁺	Electro-reduction	Carbon fiber cloth	Pt-coated Ti panel	[63]
Cd ²⁺ ; Cu ²⁺ ; Zn ²⁺ ; Ni ²⁺ ;	Electro-oxidation	Ti/RuO ₂ –IrO ₂	Ti/RuO ₂ –IrO ₂	[64]
Fe ²⁺ ; Pb ²⁺ ; As ³⁺				
Hg ²⁺	Electro-reduction and ion exchange	Graphite particle	Ti substrate	[65]
Cd ²⁺	Electro-reduction	PSAC	Graphite felt	[66]
Cu ²⁺	Microbial electrolysis cells	Stainless steel mesh	Graphite fiber brush	[67]
Cu ²⁺	Electrodeposition	Ti		[68]
Pd ²⁺ ; Zn ²⁺ ; Cd ²⁺ ; Cr ⁶⁺	Electrodeposition	Ti		[33]
Cu ²⁺ ; Ni ²⁺ ; Hg ²⁺				
Cu ²⁺	Electrocoagulation	Conductive carbon cloth	Pt-coated panel	[69]
Cu ²⁺ ; Ni ²⁺ ; Fe ²⁺	Electrolysis	Mesh Ti stainless steel plate	Mesh Pt-coated titanium	[70]
Cu ²⁺ ; Zn ²⁺ ; Pb ²⁺	Microbial electrolysis cell	Carbon cloth	Graphite brush	[71]
Ni ²⁺	Electrolysis	Graphite plate	Graphite felt	[72]
Cu ²⁺	Electrolysis	Granular graphite		[73]
Pd ²⁺ ; Ni ²⁺	Electrolysis	Cu sheet	Pt wires	[74]
Cu ²⁺ ; Cr ⁶⁺ ; Ni ²⁺	Electrodialysis	Pt	Pt	[75]
Cu ²⁺	Electrolysis	Stainless steel	Ti grid	[76]

Capacitive deionization (CDI) is among emerging separation technologies for removing charged ions from wastewater using electrochemical principles on electrode surfaces. Figure 2 shows the mechanism of CDI for HM removal. Ions are removed from the aqueous solution and are stored on the internal surface areas of the porous electrodes; this results in an effluent product stream with reduced ion concentration. Moreover, ions can be reversed into solution by reducing or even reversing the applied voltage, resulting in a product stream concentrated in ions. In principle, CDI is based on the electrosorption of cations and anions on the electrode surface captured by electrical double layers [77]. Generally, the electrical properties of electrodes govern the adsorption capacity, chiefly specific capacitance, and their surface areas are believed to be closely related to the removal efficiency

of CDI cells [78]. The CDI process may specifically remove heavy metal ions using an electric field without adding any chemicals, making the process an energy-efficient technology compared with distillation and reverse osmosis. In recent decades, CDI has grown substantially, considering electrode materials, cell configurations, and process analysis, while parasitic reactions and a relatively low desalination capacity hinder the practical application and further development of CDI [79]. Its side reactions mainly include anode oxidation reactions (such as carbon electrode oxidation and chloride oxidation), cathode reduction reactions (such as oxygen reduction and carbon electrode reduction), and co-ion expulsion (-i.e., ions with similar charge to the electrodes are expelled from the electrodes during the charging process in CDI). These reactions often occur during the operational process, increasing energy loss and leading to water quality fluctuations. The low desalination capacity is mainly due to the relatively low physical charge storage capacitance of the electrode materials and the adverse effects of side reactions. CDI technology is energy efficient, has a low life-cycle cost, is capable of removing a wide range of ionic contaminants, has a high recovery rate, and is cost-competitive compared with membrane filtration processes such as reverse osmosis (RO), which can be especially beneficial for saline groundwater treatment for rural or remote communities [78–80].

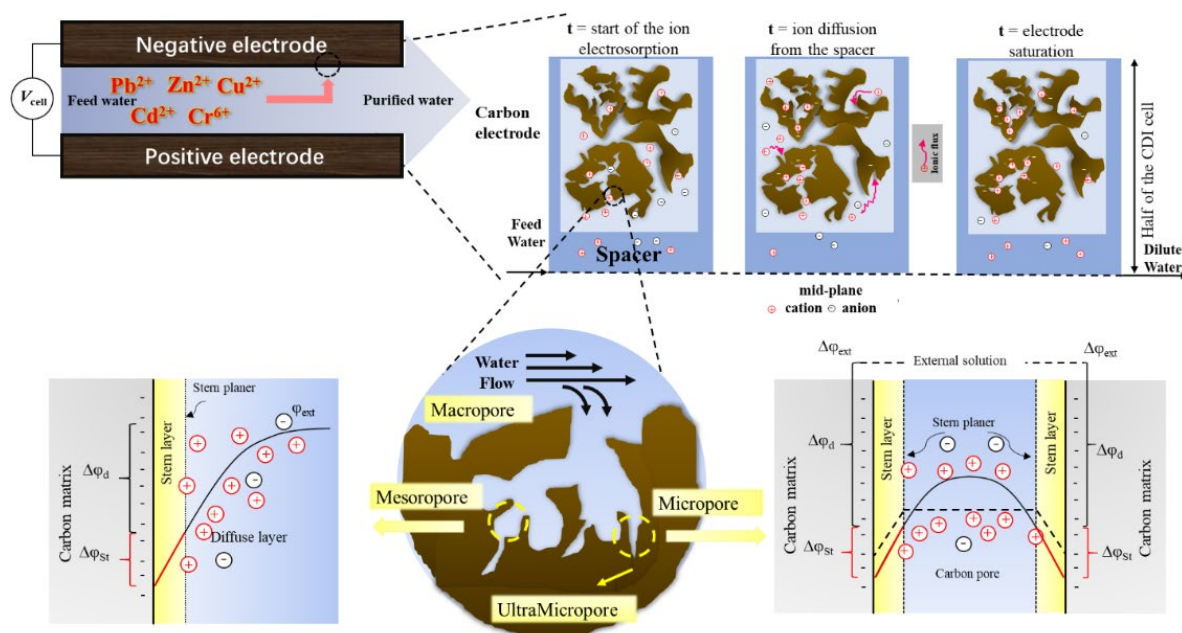


Figure 2. Summary of the mechanism of CDI for heavy metal removal.

3. Materials for Heavy Metal Removing Using CDI

Great efforts to solve the challenges of CDI have been made. These include CDI configuration optimization and developments in operation style as well as the search for highly efficient and cheap electrode materials with high adsorption capacity and stability [81]. The electrode material is a crucial component of CDI cells that determines the desalination performance of CDI [78]. Usually, electrode materials should be conducive to a high surface area and have a good affinity with heavy metal ions. A large number of electrode materials have been developed for CDI. Figure 3 summarizes the materials applied for CDI, the majority of which include carbon materials, metal oxides, polymers, and their composites.

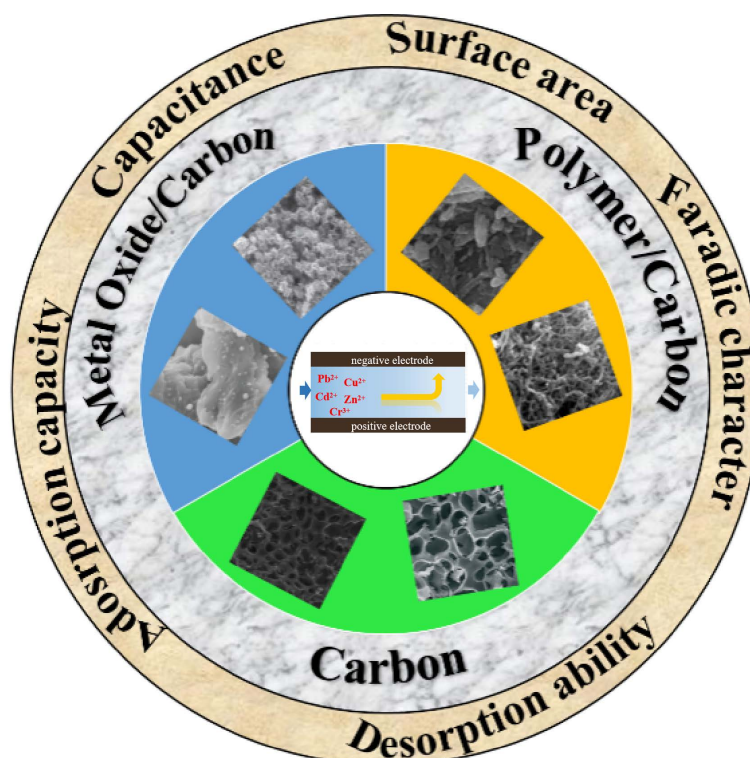


Figure 3. Summary of materials applied for CDI.

3.1. Pure Carbon Materials

Generally, adsorption capacity is governed by the electrical properties of electrodes, especially specific capacitance, and surface area is believed to be relevant to the removal efficiency of CDI cells [82]. Carbon has abundant allotropes and has been extensively studied in the past several decades for a variety of applications. Owing to its high surface area, excellent conductivity, and tunable structure, carbon materials are the most popular materials applied for CDI electrodes. Large surface areas and mesoporous carbon materials exhibit good characteristics and excellent performance regarding electrochemical activity, the adsorption/sorption of toxic gases, and the removal of HMs [83].

Carbon materials can reversibly adsorb and desorb significant amounts of HMs using double-layer mechanisms without affecting their mechanical and electrical properties. Specific surface areas and pore sizes were found to closely correlate with ion electroadsorption at the electrical double layer [84]. High-surface-area porous electrodes must be optimized for both high surface area (capacity) and pore size (kinetics), and electrosorption performance was found to be primarily determined by hydrated size, ionic charge, and initial molar concentration in solutions. Nanoporous carbons are used as a key component in the electrosorption process due to their good electrical conductivity, high surface area, and remarkable sorption capacity. Carbon aerogels, activated carbons, carbon nanofibers, carbon nanotubes, graphene, mesoporous carbon, and carbon-based composites are recognized as promising electrodes for CDI [78]. Since the first report on the electroadsorption of Cr(VI) using carbon aerogel electrodes in 1997, increasing attention has been paid to developing new carbon-based materials for heavy metal electroadsorption [85].

Activated carbon is a notable material used for electrosorption because of its strong mechanical stability; large pore volume; high surface area; electrochemical stability; and low manufacturing cost. Many investigations have revealed that activated carbon is effective in removing ions such as Na, Mg, Ca, Cl, etc., from water. For example, in one study, the removal efficiencies were 32%, 43%, and 52% for Cd^{2+} , Pb^{2+} , and Cr^{3+} , respectively, initially formed heavy metal-containing water with a concentration of 0.5 mM [86]. Electrosorption rates and ionic hydrated radii were not linear for heavy metal but in the order $\text{Cu}^{2+} > \text{Pb}^{2+} > \text{Cd}^{2+}$, attributed to the complex mechanisms occurring in electrosorption, such

as electrodeposition, and OH^- complex formation during charging [86]. Cu^{2+} and Pb^{2+} showed notably low desorption efficiency during electrode regeneration, implying high fouling potential during CDI treatment because of the facial deposition of Cu (+0.34 V) and Pb (−0.13 V). Chen et al. investigated the electrosorption and reduction behavior of Cu^{2+} and Zn^{2+} in a wide voltage window on activated carbon fiber electrodes [87]. It was shown that removal of Cu^{2+} worked better than that of Zn^{2+} at 0.4–0.6 V, while better removal efficiency for Zn^{2+} occurred in the range 0.8–1.2 V in wastewater containing a single metal ion. During the membrane CDI process, Cu^{2+} could be preferentially electrodeposited while Zn^{2+} reduction was prevented at the voltage of 0.8 V [87]. As(III) and As(VI) removal action is known, and the removal capacity of activated carbon electrodes strongly depends on applied voltage and initial arsenic concentration. The sorption capacity for treating As(V) is superior to that for As(III) due to the negative charges of prevalent As(V) species. The removal of As(V) occurs mainly via electrosorption, whereas As(III) removal using the CDI system involves the oxidation of As(III) to As(V) before it is electrostatically adsorbed on the anode surface [88]. The fundamental behavior of Cu^{2+} removal in the CDI process over activated carbon electrodes has been investigated [89]. It was shown that electrical double-layer charging assisted Cu^{2+} removal, and electrodeposition can be curbed at a low applied voltage. The equilibrium electrosorption capacity of Cu^{2+} was 24.57 mg g^{-1} by the electrical double layer at a charge potentially less than 0.8 V, while electrodeposition of Cu was seen when the potential was over 0.8 V.

The adsorption capacity of electrodes also depends on co-existing organic and inorganic pollutants. Cr(VI) electroadsorption was raised from 155.7 to 190.8 mg g^{-1} when KCl concentration inclined in an electrolyte in the range of 100 – 500 mg L^{-1} , but notably declined to 90.2 mg g^{-1} when the KCl concentration reached 1000 mg L^{-1} . High Cr^{6+} removal efficiency occurred in the absorption of Cr(VI) onto electrodes, the reduction of Cr(VI) into Cr(III), and the formation of precipitation onto the electrode surface [90]. Co-existing Sr and Cs ions in aqueous solution largely inhibited the removal efficiency of Co ions from 36.54% to 8.37% [91]. Wang et al. used a carbon aerogel as the electrode for the CDI removal of Cu^{2+} [92]. The 3D network-like carbon structure was composed of small particles with mesopores and macropores having a pore volume of $3.41 \text{ cm}^3 \text{ g}^{-1}$ nm in the carbon materials and had a great impact on the adsorption of diverse ions and the anion adsorption effect in the following order: $\text{SO}_4^{2-} > \text{NO}_3^- > \text{Cl}^-$. The highest specific capacity of 156 F g^{-1} in 6 M KOH solution, reaching a Cu^{2+} adsorption rate of 29.7 mg g^{-1} , was achieved in an optimized condition in which the Cu^{2+} concentration was 100 mg L^{-1} and the applied voltage was 1.2 V .

Graphene is a two-dimensional material with a high specific surface area and intrinsic electrical conductivity along with mechanical robustness. It is considered an excellent candidate for CDI electrodes. Graphene-based materials have been widely studied for water desalination [93,94]. However, graphene sheets are prone to stack and agglomerate, resulting in low surface area and uncontrollable pore size. This decreases the electrical double layer capacitance of the electrodes and reduces the CDI performance [95]. Zhang et al. fabricated carbon nanotube–graphene hybrid aerogels as electrode materials through the CO_2 supercritical drying of graphene–CNT hybrid hydrogel [96]. This novel material has the impressive properties of a large surface area ($435 \text{ m}^2 \text{ g}^{-1}$), large pore volume ($2.58 \text{ m}^3 \text{ g}^{-1}$), high conductivity (7.5 S m^{-1}), and being light weight (41.1 mg cm^{-3}). The hierarchically porous structure was found to be crucial to the electro-binding of four different HMs with adsorption capacities of 104.9 mg g^{-1} for Pb^{2+} , 93.3 mg g^{-1} for Hg^{2+} , 64 mg g^{-1} for Ag^+ , and 33.8 mg g^{-1} for Cu^{2+} [96]. Graphene-oxide-modified carbon felt electrodes have been used to dispose of both low-concentration and high-concentration heavy metal pollution using either direct current (DC) or alternating current (AC) electrodeposition. Graphene oxide (GO) provides a high density of surface oxygen functional groups (C–O, COOH, COH, etc.) to assist in electrodeposition. The electrodeposition method showed a capacity two orders of magnitude of a higher capacity ($>29 \text{ g}$ heavy metal for 1 g of GO) than traditional adsorption methods [97]. DC electrodeposition with GO-modified carbon

felt electrodes can reduce single-heavy-metal-ion pollution (Cu, Cd, and Pb) and multiple ion mixtures to below safe water drinking water levels. By tuning the AC frequency and voltage, the electrodeposition method can further selectively recover Cu, Cd, and Pb separately, which adds value to the heavy metal removal process [97].

Based on the electroadsorption theory, the Helmholtz electrical double layer model is widely understood [98]. The initial CDI models for EDL structure models are the Helmholtz EDL model and the Gouy–Chapman–Stern (GCS) EDL model. An advanced equilibrium EDL structure model named the modified Donnan (mD) model can account for the macropores' confined nature in CDI electrodes [99]. In the mD model, micropores are seen to have a strongly overlapped double layer, so the classical Donnan notion of a uniform pore electrostatic potential can be used. In-depth research has found that a high ion adsorption capacity is closely related to the micropores rather than the mesopores [100,101]. Thus, porous carbon is an attractive material for the electrochemical adsorption of HMs. In these micropores, typically, the Debye length λ_D is of the order of, or larger than, the pore size. In micropores, when the R of the pores is smaller than the Debye length, an overlap of the electrical double layer is found. Hence, the electrical potential makes a distinct jump from a value on the surface outside the particles to another value in the micropores [80,102]. Then, the concentration of counterions is significantly higher than that on the outside surface. Thus, the micropores (<2 nm) are highly effective in achieving high ion adsorption.

3.2. Heteroatom Doped Carbon

Heteroatom doping is the process of substituting some carbon atoms with other atoms in the carbon structure, primarily P block elements [103]. Bringing heteroatoms (e.g., N, B, S, P, etc.) into carbon nanomaterials can alter the electron configurations of the adjacent carbons due to their sizes and electronegativity differences, hence enhancing electrical conductivity and wettability [103,104]. Moreover, this process can induce a huge number of defects, which can create a more accessible surface area and is beneficial for charge accumulation.

A sheet-like N, O-enriched hierarchical porous carbon material was developed by Zhao et al. [105], adopting eggplant as the carbon source and KHCO_3 as the activation agent. The largest capacitance was up to 172.5 F g^{-1} in NaCl solution. Pb^{2+} - and Cd^{2+} -containing wastewater mainly occurred due to a high concentration of N-doped oxygen functional groups on the surface and a 3D porous structure leading to greater mass transport efficiency and electroconductibility [83]. Further, with wastewater containing Pb^{2+} and Cd^{2+} at concentrations of 0.5 ppm and 0.1 ppm, removal rates of 99.1% and 97.9%, respectively, were achieved in rechargeable Zn–air battery-coupled CDI devices. The self-powered system displayed excellent charge efficiency (60.3%) for CDI, whereby the residual concentrations of Pb^{2+} and Cd^{2+} in water dropped to 4.5 ppb and 2.2 ppb in 90 minutes. In another study, 3D honeycomb-like porous carbon was synthesized via the hydrothermal carbonization of corncob combined with KOH activation [106]. The newly prepared porous carbon-based electrodes exhibited a high capacitance of 452 F g^{-1} in 1 M Na_2SO_4 . A batch-mode CDI experiment demonstrated the removal of Cr^{6+} through a non-faradic process, achieving a removal rate of 91.85% when the initial Cr^{6+} concentration was 30 mg L^{-1} . Moreover, a highly porous N-doped graphene-based CDI device exhibited high removal efficiency (90–100%), fast removal (<30 min), and good regeneration performance (10 cycles, 99% retention) for multiple HMs (Pb^{2+} , Cd^{2+} , Cu^{2+} , Fe^{2+} , etc.) in water at a wide range of concentrations (0.05–200 ppm) [94]. Chen et al. developed an N-doped graphene nanosheet material via the one-step pyrolysis of a graphene oxide and cyanamide mixture [94]. Mamaril et al. developed an N-doped and fluorine co-doped graphene oxide as an electrode material, and a specific capacitance of 245.6 F g^{-1} was achieved with a high removal percentage of 95% and a specific electrosorption capacity of 52.4 mg g^{-1} at 100 mg L^{-1} Cu(II) [107]. It is worth noting that highly prepared porous carbon was firstly used as an electrode for membrane CDI to remove multiple HMs, e.g., Pb^{2+} , Cd^{2+} , Fe^{2+} , and Cu^{2+} , simultaneously, as the prepared carbon material showed a high specific surface area of

$695 \text{ m}^2 \text{ g}^{-1}$. At 200 ppm, the adsorption capacity of NG for Pb^{2+} and Cd^{2+} can, dramatically, reach 521 mg g^{-1} and 498 mg g^{-1} , and high removal efficiencies of 96%, 80%, 100%, and 100% for Fe^{2+} , Cd^{2+} , Pb^{2+} , and Cu^{2+} , respectively, have been achieved with a wide range of initial concentrations (0.05–200 ppm).

Wang et al. developed a three-dimensional reduced graphene oxide/nitrogen-doped carbon quantum dot composite. In this work, the electrosorption capacity of an rGO/25% NCDs electrode was 19.26 mg/g when the initial concentration of Pb^{2+} was 5 mg/L [108]. Hu et al. developed two kinds of N-doped carbon with distinct configurations: pyrrolic N-dominated graphene (N-5-G) and pyridinic N-dominated graphene (N-6-G) [109]. The specific capacitance of N-6-G is 239.7 F g^{-1} , which is larger than N-5-G (195.2 F g^{-1}) in Na_2SO_4 solution, while the Pb^{2+} electrosorption capacity of N-5-G is 2.43 mg m^{-2} , which is three times that of N-6-G (0.73 mg m^{-2}). The removal efficiency of Pb^{2+} was found to be 95.8% for N-5-G. Three main types of nitrogen defects exist in the N-doped carbon structure: graphitic nitrogen, pyridinic nitrogen, and pyrrolic nitrogen. The final two kinds are proven to be more electroactive for CDI than graphitic nitrogen because they are prone to donor electrons [109]. Graphitic nitrogen and pyridine nitrogen oxide have shown merit in capacitance. Hu et al. revealed that pyridinic nitrogen groups tend to prefer H^+ and Na^+ , while pyrrolic nitrogen exhibits efficient Pb^{2+} sorption. This conclusion bridges the matrix structure of N-doped carbon with CDI performance for the removal of heavy metal ions.

P and N have the same number of valence electrons, meaning that P-doped carbon materials are also electron-rich. Moreover, the diameter of P is much larger than that of C; thus, P-doping results in the greater local structural distortion of the hexagonal carbon framework and also protrudes out of the graphene plane. The reasons why P-doped carbon materials overcome the steric hindrance effects encountered in N-doped carbon materials were indicated in [110]. Interestingly, multi-heteroatom co-doped carbon materials can produce double functional groups or diatomic synergies, likely resulting in improved electrical conductivity and the enhanced wettability of the carbon materials. The doping of nitrogen atoms into graphitic networks is seen as one of the best approaches to producing n-type conductive materials with improved conductivity [109].

3.3. Polymer Functionalized Carbon Materials

The selectivity of materials for electrochemical adsorption has been highlighted because high selective adsorption can simultaneously achieve the separation and recovery of valuable heavy metals. Despite their large number of functionalities, the inhomogeneous surface properties of carbon materials mean that they mostly exhibit poor selectivity. Functionalization of the carbon surface with designed functional groups not only provides high-density homogenous functional groups but can control the selective chelation of functional groups with designed heavy metal species. Ethylene diamine tetraacetic acid (EDTA) and 3-aminopropyltriethoxysilane functionalized 3D graphene were applied to selectively remove Na(I) and Pb(II) [111]. Interestingly, Na^+ ions were electrically adsorbed on the 3D graphene pores by electrosorption, while Pb^{2+} ions were adsorbed on a EDTA-grafted macroscopic 3D graphene cathode (3DEGR) via a chelation reaction. At pH 6.0, using synthetic wastewater containing 20 ppm Pb^{2+} and 100 ppm Na^+ , the removal efficiency for Pb^{2+} was 99.9% and the desorption rate was ~99.6%. The removal efficiency remained at 94.4% after eight cycles, demonstrating the high reversibility of these materials. Thus, heavy metal and salt ions could be separated and recovered, purifying wastewater [111]. The adsorption/desorption experiments indicated that the specific adsorption capacity of the composite for Cu^{2+} was 99.67 mg g^{-1} . Moreover, polypyrrole/chitosan/CNT (Py/CS/CNT) nanomaterials were prepared via in situ polymerization [112]. The modified nanomaterials provided sufficient porosity for the diffusion of ions and solvent molecules. In the CuSO_4 solution of 100 mg L^{-1} , a higher Cu^{2+} removal rate of 80% was achieved compared with Py/CS-coated electrodes (56.4%). The decreased capacitance of Py/CS/CNT was only 3.4% after 50 cycles, showing remarkable stability due to the highly conductive CNTs which provided an electron pathway and stabilized the polypyrrole and chitosan. Shi et al. used

the air-plasma method to modify the structure and composition of polytetrafluoroethylene/carbon nanotube composite materials [113]. Plasma activation raised the relative O and N content, which improved the Pb^{2+} removal capacity from 1.36 mg g^{-1} to 2.40 mg g^{-1} at a voltage of 450 mV and initial concentration of 5 mg L^{-1} .

3.4. Metal Oxide Supported Carbon Composites

Many solutions have been developed to solve the aforementioned challenges. For example, one of the best of such solutions involves using faradaic electrode materials as the electrode. Unlike non-faradaic materials such as porous carbon electrodes, which store salt ions capacitively in an electric double layer along surfaces or nanopores, faradaic electrodes store ions via intercalation or conversion reactions [114]. Incorporated transitioned metal oxide could efficiently enhance the capacitance and electrosorption ability of carbon-based materials due to the conversion of heavy metal ions and the adsorption of HMs on defects as well as the intercalation of metal ions into the metal oxide layer structure. Banat et al. synthesized highly mesoporous peanut-shell-derived activated carbon/ Fe_3O_4 nanocomposite materials [115]. Cr(VI) was reduced to Cr(III) by Fe(II) ions of Fe_3O_4 and was then directly electro-captured on carbon-based composite materials in acidic conditions. The synergetic effect of both physical adsorption and electrosorption combined with a reduction pathway was crucial to Cr(VI) removal. Nearly 99.9% of the Cr(VI) was removed with a high electroadsorption rate up to 24.5 mg g^{-1} at pH 6.5 with an initial concentration of 50 mg L^{-1} . Wang et al. induced highly distributed $\alpha\text{-Fe}_3\text{O}_4$ of a uniform size on carbon matrixes through the carbonization of MIL101(Fe) [116]. The porous carbon yield exhibited surface areas of $\sim 1832 \text{ m}^2 \text{ g}^{-1}$ and showed excellent adsorption capacity for Pb^{2+} (830.17 mg g^{-1}) and a high removal efficiency of 90.3% at an initial concentration of 500 mg L^{-1} Pb(II)-containing water through the CDI process with high durability within 10 cycles [116]. This high adsorption capacity and removal efficiency resulted from the electroadsorption and electrodeposition of the Pt(II) on the electrode [116]. In another study, a graphene sheet exfoliated by potassium ions from graphite was prepared [117]. Fe_3O_4 nanoparticles were successfully supported on porous graphene sheets via the hydrothermal process. The Fe_3O_4 /porous graphene nanocomposites showed great potential for the removal of both organic pollutants and heavy metal ions, with the removal rates for Pb^{2+} , Cu^{2+} , and Cd^{2+} found to be 90.6%, 92%, and 90.2%, respectively. Moreover, the results revealed ultrahigh electrosorption capacities for Pb^{2+} , Cu^{2+} , and Cd^{2+} ions which were found to be 47, 40, and 49 mg g^{-1} , respectively, in NaCl solution with an initial concentration of 500 mg L^{-1} , a cell potential of 1.6 V, and a 0.03 mM initial metal ion concentration. $\alpha\text{-MnO}_2$ nanoneedles were grown on carbon fiber paper using an ordinary hydrothermal method [118]. Both Ni(II) and Mn(II) ions reduced easily and electrosorbed on the $\alpha\text{-MnO}_2$ -carbon-paper-based electrode due to its mesoporous structure, contributing to fast electron charge transfer. Birnessite-type MnO_2 on carbon nanotubes can effectively remove both Zn^{2+} and Ni^{2+} via constant potential electrolysis. CNTs offer a larger specific surface area and higher conductivity to birnessite. Their removal capacities for Zn^{2+} and Ni^{2+} have been found to reach 155.6 and 158.4 mg g^{-1} in 50 mg L^{-1} origin wastewater, respectively. Hexagonal birnessite is proposed to consist of edge-sharing Mn(IV)O_6 octahedral layers, and these layers are interlayered with water molecules. There are Mn(IV) vacancies in Mn(IV)O_6 octahedral layers due to the repulsion between neighboring Mn(IV). Heavy metal ions can be adsorbed on or below the vacancies during the isothermal adsorption process [119]. Figure 4 depicts the mechanisms of metal-oxide-supported carbon composites in heavy metal removal. GO- TiO_2 nanotube composites have high specific electrosorption capacities of 253.25 mg g^{-1} and 241.65 mg g^{-1} for Cu^{2+} and Pb^{2+} , respectively [120]. This microwave-assisted fabricated composite releases little during desorption at zero voltage caused by induced oxygen, and π electrons lead to strong interactions with Pb^{2+} and Cu^{2+} . Metal oxide/carbonaceous gel hybrid materials derived from natural and renewable biomass exhibit excellent flexibility and high electrochemical reactivity (capacitance of 120.4 F g^{-1} in 50 mg L^{-1} CuCl_2 solution), primarily in the area of CDI decontamination applications. In

one study, Cu^{2+} was nearly completely removed (removal capacity of 57.3 mg g^{-1}) and the as-assembled CDI testing apparatus showed durability after 1000 cycles [121]. Activated carbon cloth coated with zinc oxide nanoparticles has been used for electrode inflow via a CDI system. Upon incorporation with ZnO NPs, electrosorption efficiency was enhanced from 17% to 33% for Pb^{2+} , from 21% to 29% for Cd^{2+} , and from 21% to 35% for mixed Pb^{2+} and Cd^{2+} ions [122]. These results together illustrate the promising applications of metal-oxide/carbon electrodes for heavy metal removal.

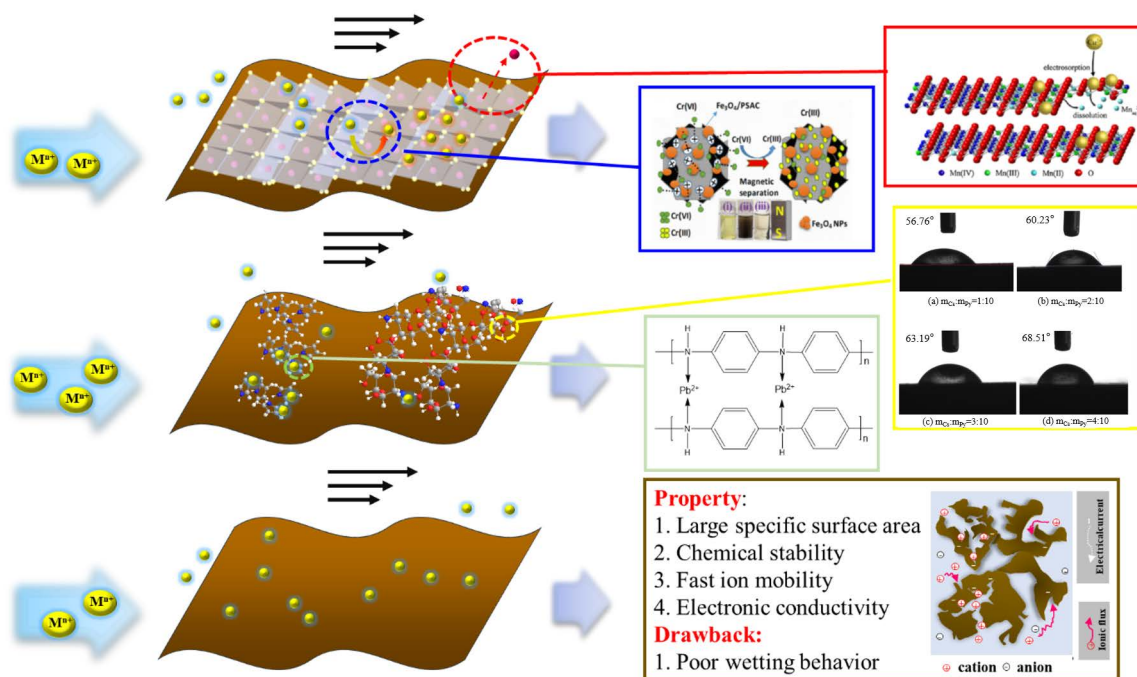


Figure 4. Mechanism of metal-oxide-supported carbon composites for heavy metal removal.

3.5. Others

Aside from carbon-based materials, polymer-based materials have attracted great interest owing to their ion-exchanging ability and conductivity. Polypyrrole is one of the most studied polymers due to its high specific capacitance, high conductivity, and simple preparation. Polyaniline/attapulgite composites (PANI/ATP) were prepared via in situ oxidative polymerization [123]. The calculated equilibrium adsorption capacity was 15.42 mg g^{-1} . The facile modified paper electrode with polymer attached to the surface of ATP contributed to the high removal efficiency of lead ions (66.5%) in wastewater, with an initial concentration of 2.5 mM Pb^{2+} and stable cyclability after 10 runs (64.2%). Li et al. deposited polypyrrole on chitosan, a stable adhesive agent functionalized with $-\text{OH}$ and $-\text{NH}_2$ groups, and proved that a polypyrrole/chitosan composite (Py/CS) exhibits considerably stable electroadsorption and desorption behavior and shows good performance regarding the removal of heavy metal ions including Ag^+ , Cu^{2+} , Pb^{2+} , and Cd^{2+} [124]. Transition metal sulfide has been viewed as a promising modified candidate for CDI. Hu et al. decorated ZnS and FeS on a carbon felt electrode. The ZnS on the carbon material increased the wettability and electrochemical capacitance. The enhanced adsorption ability of Cu^{2+} and removal capacity of Cu^{2+} was 27.4 mg g^{-1} in the presence of Cr^{6+} and natural organic matter [124].

The materials used for heavy metal electrosorption are primarily carbon-based materials due to their tunable properties such as surface area, pore size, and distribution as well as their surface functionalities. Overall, polymer carbon composites have been investigated for Cu and Pb removal, and their physical and chemical adsorption abilities were found to be excellent owing to the chelation process of capturing ions. However, a few unusual properties, such as restricted specific area and relatively poor conductivity, limit their per-

formance regarding the electrosorption of HMs. Their adsorption capacity is relatively low, and a higher adsorption capacity was achieved for Pb using PTFE/CNTs. An adsorption capacity of 16.83 mg g^{-1} for Cu was achieved using polypyrrole/chitosan/CNT due to the use of functional polymer-like polypyrrole, a common conducting polymer, which showed ultra-high specific capacitance and conductivity [112,113]. Moreover, synergy between polypyrrole and chitosan increased adsorption capacity through the chelation process [125,126]. Metal-oxide carbon composites have been proven to show excellent performance in the removal of Pb, Cu, and Cr. Fe_3O_4 /peanut-shell-derived activated carbon material exhibited a 99.9% removal rate and 24.5 mg g^{-1} Cr^{6+} adsorption rate in wastewater [116]. The redox ability of transition metal oxide was useful in deducing the toxicity of HMs during the electrosorption process. The removal of Cu by MnO_2 /carbon fiber demonstrated a 96% removal rate with a 172.9 mg g^{-1} adsorption rate [127]. The enhancement of adsorption via the polarization potential and unique nanoflower microstructure of deposited MnO_2 may equally lead to the superior adsorption ability of MnO_2 /CF electrodes. TiO_2 -nanotube-coated CNT electrodes have been proven to efficiently remove Cu and Pb with adsorption capacities of 282.25 mg g^{-1} and 241.65 mg g^{-1} , respectively. The excellent activity of metal oxide/CNT composite relies on its mesoporous features, good ion-exchanging properties, and very high conductivity. The removal rates and adsorption capacities for Pb by Fe_2O_3 /C were 90.3% and 830.17 mg g^{-1} , respectively; this improvement was accredited to its considerably large specific surface area ($1832 \text{ m}^2 \text{ g}^{-1}$) and high dispersion at the near quantum scale. Carbon has been shown to be an excellent material for various HMs, including Pb, Cu, Cr, Cd, and Ni. Carbon is the most widely applied material due to its abundance in nature and facile modification methods. Table 2 presents the various materials that have been studied for heavy metal removal, such as activated carbons, carbon cloths/fiber, ordered mesoporous carbons, carbon aerogels, carbide-derived carbons, carbon nanotubes, carbon black, and graphene.

Table 2. CDI methods for heavy metal removal.

Metal	Working Electrode	Counter Electrode	Removal Rate/Adsorption Rate/CF	Ref
Cr^{6+}	Fe_3O_4 /peanut-shell-derived activated carbon	PSAC	99.9%; 24.5 mg/g ; 610 F/g	[116]
Pd^{2+} , Cd^{2+}	Eggplant-derived carbon	Zn foil	99.1% Pd; 97.9% Cd; 172.5 F/g	[105]
Pb^{2+}	Fe_2O_3 @C	Fe_2O_3 @C	90.3%; 830.17 mg/g ; 115.6 F/g	[116]
Cu^{2+}	Polypyrrole/chitosan		56.4%; 99.67 mg/g ; 102.96 F/g	[124]
Cu^{2+}	Polypyrrole /chitosan /CNT	Graphite	80.08%; 16.83 mg/g ; 103.19 F/g	[112]
Cu^{2+}	ZnS-decorated carbon felt		>90%; 27.4 mg/g ; 168 F/g	[128]
Cr^{6+}	Bael-fruit-shell-derived carbon on Cu wire	Fe wire	100%; -; -	[129]
Pd^{2+}	Graphite foil		90%; -; -	[130]
Cu^{2+}	Activated carbon on Ti net		95.7%; -; -	[131]
Pd^{2+} , Cd^{2+}	rGo-CNT on Ti platcocoe	Pt plate/sheet	253.25 mg/g Cu , 241.65 mg/g Pb ; 165.22 F/g	[120]
Cr	MIL-53(Fe) on graphite paper	Graphite paper	72.2% ; 224.7 F/g	[132]
Cr^{6+}	Corncob-derived 3D porous carbon on Ni foam	Pt foil	91.85% ; 452 F/g	[106]
Pb^{2+} , Cd^{2+} , Cu^{2+} , Fe^{2+}	N-doped graphene on graphite foil paper	Graphite rod	90~96%; 521 mg/g Pb ; 498 mg/g Cu	[94]
Zn^{2+} , Ni^{2+}	$\text{Na}_4\text{Mn}_{14}\text{O}_{27}$ on carbon fabric	Carbon fabric	90% Zn; 88% Ni 155.6 mg/g Zn ; 158.4 mg/g Ni	[119]
Pb^{2+} , Cu^{2+} ; Cd^{2+}	Fe_3O_4 /graphene		90.6% Pb; 92% Cu; 90.2% Cd	[117]
Cu^{2+}	TiO_2 /watermelon derived carbonaceous hydrogels		57.13 mg/g ; 120.4 F/g	[121]
Cd^{2+} ; Pd^{2+} ; Cr^{6+}	Activated carbon cloth on stainless mesh	Activated carbon cloth on stainless mesh	81% Pb; 78% Cr; 42% Cd	[133]

Table 2. Cont.

Metal	Working Electrode	Counter Electrode	Removal Rate/Adsorption Rate/CF	Ref
Pb ²⁺	3D macroscopic graphene on graphite paper	3D N-doped macroscopic graphene on graphite paper	99.6%; 134.4 F/g	[111]
Mn ²⁺	Graphene-chitosan-Mn ₃ O ₄	Pt foil	12.7 mg/g; 190 F/g	[134]
Cu ²⁺	Activated carbon	Activated carbon	69%; 24.57 mg/g; 164.3 F/g	[89]
Pb ²⁺ , Hg ²⁺ , Ag ⁺ , Cu ²⁺	Graphene/MWCNT hybrid aerogels on Ni foam	Graphene/MWCNT hybrid aerogels on Ni foam	104.9 mg/g Pb; 93.3 mg/g Hg; 64 mg/g Ag; 33.8 mg/g Cu	[96]
Ni ²⁺ , Mn ²⁺	α-MnO ₂ /carbon fiber paper	Active carbon	88.9% 16.4 mg/g Ni; 98.5% Mn; 126.7 F/g	[118]
Cu ²⁺	Carbon aerogel	Carbon aerogel	73.6%; 29.7 mg/g; 156 F/g	[92]
Pb ²⁺	N-doped graphene	Carbon cloth	95.8%; 2.43 mg/m ² ; 195.2 F/g	[109]
Pb ²⁺	Chicken-feather-derived carbon	Chicken-feather-derived carbon	81%; 4.1 mg/g	[135]
Co ²⁺	Activated carbon cloth	Activated carbon cloth	36.54%; 8.3 mg/g	[91]
Cu ²⁺	Activated carbon fibers		108.8 mg/g Cu; 122.6 mg/g Zn	[87]
Pb ²⁺	PTFE/CNTs		2.40 mg/g; 43 F/g	[113]
Pb ²⁺	Polyaniline/attapulgit		66.5%; 12.39 mg/g	[123]
Cu ²⁺	MnO _x	Saturated calomelelectrode	66%; 372.3 mg/g (electro sob) 44.3 mg/g (iso sorb)	[136]

4. Challenges and Opportunities

Heavy metal removal using CDI techniques provides an energy-efficient and cheap removal method. This real application can be integrated into renewable energy systems, which would be useful in remote areas. Studying the literature on the assessment of CDI energy efficiency reveals its relatively low, specific energy consumption, which is considerably below 1 kWh m⁻³. Theoretically, energy is stored in the electrical double layer during the charging process, whereby it may be discharged and recovered. However, practically, resistance during charge and discharge leads to energy losses. This resistance arises from the contact resistance of components, connecting wires, the electronic resistance in the solid matrix of the electrode, and ionic transportation resistance. Hence, this requires the optimization of electrode material composition, structure, and porosity as well as minimized contact resistance in the whole CDI assembly.

The pursuit of intercalation materials as promising CDI electrode materials is primarily driven by their ability to yield far higher specific adsorption capacities than conventional carbon-based electrodes. This is due to the ability of intercalation materials to store ions in their solid phase, in contrast to carbon electrodes that store ions by forming EDLs in their micropores. In theory, intercalation materials do not possess a direct advantage over carbonaceous materials considering the reduction in cell resistance and resistive energy loss. Most intercalation materials have poor electronic conductivity, which is inimical to high energy efficiency. However, these materials have two major advantages that allow im-CDI systems to operate in ways that significantly benefit TEE. The first advantage is their high specific adsorption capacity. Although specific adsorption capacity is not directly relevant to TEE, the high SAC of intercalation materials enables im-CDI to remove a considerable amount of salt and thereby achieve an appreciable salinity percentage reduction when employed to desalinate high-salinity feed solutions.

CDI requires an electrode with a large ion-accessible specific surface area. Metal ion electrosorption is a surface-related process, and surface area plays a very important role. However, the entire surface may not have access to metal ions; the latest research shows that not all BET surface areas can participate in ion adsorption. Van der Waals results have revealed that the effectively used are of a porous activated carbon electrode is ~55% of the

BET area of the electrode. The wettability of the electrode and the porous structure of the materials ensure a greater surface area is engaged in ion charge and discharge. Notably, the specific area is highly dependent on the number of small pores, while more small pores limit ion transportation. The final and ultimate limitation on pore size is the metal ion size. Moreover, large pores provide better transportation pathways but limit surface area, while small pores provide a large surface area and higher adsorption capacity but are constrained by ion transportation.

The relationship between these two factors raises vital questions regarding the validity of the gas adsorption models usually used to determine porous electrode surface areas and pore size distributions as well as the effective sizes of ions in pores concerning their degree of solvation. For instance, it is important to discover to what extent and at which potentials the solvation shells of ions entering into pores are partially or completely removed. For example, Li et al. reported an order of Fe^{3+} (0.62 mg FeCl_3/g) > Ca^{2+} (0.55 mg CaCl_2/g) > Mg^{2+} (0.52 mg MgCl_2/g) > Na^+ (0.45 mg NaCl/g) for mono-component solutions, while the order became $\text{Na}^+ > \text{Mg}^{2+} > \text{Ca}^{2+} > \text{Fe}^{3+}$ in mmol/g [137]. Moreover, the removal of certain HMs by CDI was complicated, and an observed order of $\text{Cr}^{2+} > \text{Pb}^{2+} > \text{Cd}^{2+}$ in the percentage removal by Huang et al. was observed under the effect of physical adsorption, which introduced uncertainties into the quantification of the sole electrosorption amount [133]. Thus, a good CDI electrode should not only exhibit good porosity and connectivity; the porosity of the electrode material should also allow for a reasonable combination with macropores, mesopores, and micropores to balance the adsorption surface area and metal ion transportation. Further, dead pores that are not accessible to the ions should be avoided.

The good electrochemical stability of a material over wide pH and voltage ranges plays a key role in real applications. The oxidation of electrode materials under electrochemical conditions is inimical to their stability. The stability of an electrode is also closely related to its high electric conductivity and contact resistance between the porous electrode and the current collector. Higher resistance leads to the generation of local heat, and thus speeds up the corrosion of carbon and the dissolution of metal species. Therefore, in addition to a low-cost design and simple scalability, the design of compacted electrodes with good processability, such as being shapeable into film electrodes based on compacted powders, fibers, or monolith film electrodes, is crucial to improving electrochemical stability.

Author Contributions: Y.X.: writing—original draft and conceptualization; Z.Z.: data curation; X.Z.: validation and visualization; Y.Z.: project administration; W.D.: supervision; Y.C.: writing—review and editing. All authors have read and agreed to the published version of the manuscript.

Funding: This research was funded by the Innovative Province Construction Special Project (2019SK2281), the National Natural Science Foundation of China (No. 42177231), and the Key Research and Development Project of Hunan Province (2019SK2291).

Institutional Review Board Statement: Not applicable.

Informed Consent Statement: Not applicable.

Data Availability Statement: Data sharing is not applicable to this article.

Acknowledgments: This work was financially supported by the Innovative Province Construction Special Project (2019SK2281), the National Natural Science Foundation of China (No. 42177231), and the Key Research and Development Project of Hunan Province (2019SK2291).

Conflicts of Interest: The authors declare no conflict of interest.

References

1. Garcés-Pastor, S.; Fletcher, W.J.; Ryan, P.A. Ecological impacts of the industrial revolution in a lowland raised peat bog near Manchester, NW England. *Ecol. Evol.* **2023**, *13*, e9807. [[CrossRef](#)] [[PubMed](#)]
2. Ali, H.; Khan, E. What are heavy metals? Long-standing controversy over the scientific use of the term ‘heavy metals’—proposal of a comprehensive definition. *Toxicol. Environ. Chem.* **2018**, *100*, 6–19. [[CrossRef](#)]
3. Odetola, L.; Sills, S.; Morrison, S. A pilot study on the feasibility of testing residential tap water in North Carolina: Implications for environmental justice and health. *J. Expo. Sci. Environ. Epidemiol.* **2021**, *31*, 972–978. [[CrossRef](#)] [[PubMed](#)]

4. Raffa, C.M.; Chiampo, F.; Shanthakumar, S. Remediation of Metal/Metalloid-Polluted Soils: A Short Review. *Appl. Sci.* **2021**, *11*, 4134. [\[CrossRef\]](#)
5. Zhou, Q.; Xue, S.; Zhang, L.; Chen, G. Trace elements and the thyroid. *Front. Endocrinol.* **2022**, *13*, 904889. [\[CrossRef\]](#)
6. Xu, Y.; Chen, R.; Zeng, Q. Ferroptosis As a Mechanism for Health Effects of Essential Trace Elements and Potentially Toxic Trace Elements. *Biol. Trace Elem. Res.* **2022**. [\[CrossRef\]](#)
7. Liu, P.; Wu, Q.; Hu, W.; Tian, k.; Huang, B.; Zhao, Y. Comparison of heavy metals in riverine and estuarine sediments in the lower Yangtze River: Distribution, sources, and ecological risks. *Environ. Technol. Innov.* **2023**, *30*, 103076. [\[CrossRef\]](#)
8. Dong, Y.; Chen, D.; Lin, H. The behavior of heavy metal release from sulfide waste rock under microbial action and different environmental factors. *Environ. Sci. Pollut. Res.* **2022**, *29*, 75293–75306. [\[CrossRef\]](#)
9. Shi, J.; Zhao, D.; Ren, F.; Huang, L. Spatiotemporal variation of soil heavy metals in China: The pollution status and risk assessment. *Sci. Total Environ.* **2023**, *871*, 161768. [\[CrossRef\]](#)
10. Ys, A.; Sz, A.; Syp, B.; Sz, A.; Yang, Y.C.; Hz, D. Performance evaluation and optimization of flocculation process for removing heavy metal—ScienceDirect. *Chem. Eng. J.* **2020**, *385*, 123911.
11. Zhao, X.; Cui, K.; Huang, K. Enhanced interfacial salt effect on extraction and separation of Er(III) from Mg(II), Al(III), Fe(III) sulfate aqueous solutions using bubble-supported organic liquid membrane. *Sep. Purif. Technol.* **2022**, *285*, 120344. [\[CrossRef\]](#)
12. Fraser, A.C.; Yankey, J.; Coronell, O.; Dingemans, T.J. A Sulfonated All-Aromatic Polyamide for Heavy Metal Capture: A Model Study with Pb(II). *ACS Appl. Polym. Mater.* **2023**, *5*, 856–865. [\[CrossRef\]](#)
13. Bazrafshan, E.; Mohammadi, L.; Ansari-Moghaddam, A.; Mahvi, A.H. Heavy metals removal from aqueous environments by electrocoagulation process—A systematic review. *J. Environ. Health Sci. Eng.* **2015**, *13*, 74. [\[CrossRef\]](#)
14. Kim, T.; Kim, T.K.; Zoh, K.D. Removal mechanism of heavy metal (Cu, Ni, Zn, and Cr) in the presence of cyanide during electrocoagulation using Fe and Al electrodes. *J. Water Process Eng.* **2020**, *33*, 101109. [\[CrossRef\]](#)
15. Tezcan Un, U.; Onpeker, S.E.; Ozel, E. The treatment of chromium containing wastewater using electrocoagulation and the production of ceramic pigments from the resulting sludge. *J. Environ. Manag.* **2017**, *200*, 196–203. [\[CrossRef\]](#)
16. Ali Maitlo, H.; Kim, K.-H.; Yang Park, J.; Hwan Kim, J. Removal mechanism for chromium (VI) in groundwater with cost-effective iron-air fuel cell electrocoagulation. *Sep. Purif. Technol.* **2019**, *213*, 378–388. [\[CrossRef\]](#)
17. Aoudj, S.; Khelifa, A.; Drouiche, N.; Belkada, R.; Miroud, D. Simultaneous removal of chromium(VI) and fluoride by electrocoagulation–electroflotation: Application of a hybrid Fe–Al anode. *Chem. Eng. J.* **2015**, *267*, 153–162. [\[CrossRef\]](#)
18. Vasudevan, S.; Lakshmi, J. Effects of alternating and direct current in electrocoagulation process on the removal of cadmium from water—A novel approach. *Sep. Purif. Technol.* **2011**, *80*, 643–651. [\[CrossRef\]](#)
19. Pocięcha, M.; Lestan, D. Using electrocoagulation for metal and chelant separation from washing solution after EDTA leaching of Pb, Zn and Cd contaminated soil. *J. Hazard. Mater.* **2010**, *174*, 670–678. [\[CrossRef\]](#)
20. Kobya, M.; Ulu, F.; Gebologlu, U.; Demirbas, E.; Oncel, M.S. Treatment of potable water containing low concentration of arsenic with electrocoagulation: Different connection modes and Fe–Al electrodes. *Sep. Purif. Technol.* **2011**, *77*, 283–293. [\[CrossRef\]](#)
21. Ahmed Basha, C.; Bhadrinarayana, N.S.; Anantharaman, N.; Meera Sheriffa Begum, K.M. Heavy metal removal from copper smelting effluent using electrochemical cylindrical flow reactor. *J. Hazard. Mater.* **2008**, *152*, 71–78. [\[CrossRef\]](#) [\[PubMed\]](#)
22. Song, P.; Yang, Z.; Zeng, G.; Yang, X.; Xu, H.; Wang, L.; Xu, R.; Xiong, W.; Ahmad, K. Electrocoagulation treatment of arsenic in wastewaters: A comprehensive review. *Chem. Eng. J.* **2017**, *317*, 707–725. [\[CrossRef\]](#)
23. de Oliveira, M.T.; Torres, I.M.S.; Ruggeri, H.; Scalize, P.; Albuquerque, A.; Gil, E.d.S. Application of Electrocoagulation with a New Steel-Swarf-Based Electrode for the Removal of Heavy Metals and Total Coliforms from Sanitary Landfill Leachate. *Appl. Sci.* **2021**, *11*, 5009. [\[CrossRef\]](#)
24. Fu, F.; Wang, Q. Removal of heavy metal ions from wastewaters: A review. *J. Environ. Manag.* **2011**, *92*, 407–418. [\[CrossRef\]](#) [\[PubMed\]](#)
25. Azimi, A.; Azari, A.; Rezakazemi, M.; Ansarpour, M. Removal of Heavy Metals from Industrial Wastewaters: A Review. *ChemBioEng Rev.* **2017**, *4*, 37–59. [\[CrossRef\]](#)
26. Al-Saydeh, S.A.; El-Naas, M.H.; Zaidi, S.J. Copper removal from industrial wastewater: A comprehensive review. *J. Ind. Eng. Chem.* **2017**, *56*, 35–44. [\[CrossRef\]](#)
27. Xue, G.; Lai, S.; Li, X.; Zhang, W.; You, J.; Chen, H.; Qian, Y.; Gao, P.; Liu, Z.; Liu, Y. Efficient bioconversion of organic wastes to high optical activity of L-lactic acid stimulated by cathode in mixed microbial consortium. *Water Res.* **2018**, *131*, 1–10. [\[CrossRef\]](#)
28. Mohtashami, R.; Shang, J.Q. Treatment of automotive paint wastewater in continuous-flow electroflotation reactor. *J. Clean. Prod.* **2019**, *218*, 335–346. [\[CrossRef\]](#)
29. Mazumder, A.; Chowdhury, Z.; Sen, D.; Bhattacharjee, C. Electric field assisted membrane separation for oily wastewater with a novel and cost-effective electrocoagulation and electroflotation enhanced membrane module (ECEFM). *Chem. Eng. Process.-Process Intensif.* **2020**, *151*, 107918. [\[CrossRef\]](#)
30. Pletcher, D.; Comninellis, C.; Chen, G. (Eds.) Electrochemistry for the environment. *J. Appl. Electrochem.* **2010**, *40*, 2203. [\[CrossRef\]](#)
31. Kozodaev, A.; Andrushko, A.; Firsova, A. Research of reagent-free waste water treatment methods of the chrome plating line for mineralizing the rod of hydraulic cylinders. *IOP Conf. Ser. Mater. Sci. Eng.* **2019**, *492*, 012021. [\[CrossRef\]](#)
32. Khelifa, A.; Moulay, S.; Naceur, A.W. Treatment of metal finishing effluents by the electroflotation technique. *Desalination* **2005**, *181*, 27–33. [\[CrossRef\]](#)

33. Tran, T.-K.; Leu, H.-J.; Chiu, K.-F.; Lin, C.-Y. Electrochemical Treatment of Heavy Metal-containing Wastewater with the Removal of COD and Heavy Metal Ions. *J. Chin. Chem. Soc.* **2017**, *64*, 493–502. [\[CrossRef\]](#)
34. Belkacem, M.; Khodir, M.; Abdelkrim, S. Treatment characteristics of textile wastewater and removal of heavy metals using the electroflotation technique. *Desalination* **2008**, *228*, 245–254. [\[CrossRef\]](#)
35. Hu, L.; Wang, F.; Balogun, M.S.; Tong, Y. Hollow Co₂P/Co-carbon-based hybrids for lithium storage with improved pseudocapacitance and water oxidation anodes. *J. Mater. Sci. Technol.* **2020**, *55*, 203–211. [\[CrossRef\]](#)
36. Krstić, V.; Pešovski, B. Reviews the research on some dimensionally stable anodes (DSA) based on titanium. *Hydrometallurgy* **2019**, *185*, 71–75. [\[CrossRef\]](#)
37. Paul, D.E.S.D. The history of progress in dimensionally stable anodes. *JOM J. Miner. Met. Mater. Soc.* **1993**, *45*, 41–43.
38. Zeradjanin, A.R.; La Mantia, F.; Masa, J.; Schuhmann, W. Utilization of the catalyst layer of dimensionally stable anodes—Interplay of morphology and active surface area. *Electrochim. Acta* **2012**, *82*, 408–414. [\[CrossRef\]](#)
39. Al-Amshawee, S.; Yunus, M.Y.B.M.; Azoddein, A.A.M.; Hassell, D.G.; Dakhil, I.H.; Hasan, H.A. Electrodialysis desalination for water and wastewater: A review. *Chem. Eng. J.* **2020**, *380*, 122231. [\[CrossRef\]](#)
40. Bolisetty, S.; Peydayesh, M.; Mezzenga, R. Sustainable technologies for water purification from heavy metals: Review and analysis. *Chem. Soc. Rev.* **2019**, *48*, 463–487. [\[CrossRef\]](#)
41. Pedersen, A.J.; Ottosen, L.M.; Villumsen, A. Electrodialytic removal of heavy metals from different fly ashes. *J. Hazard. Mater.* **2003**, *100*, 65–78. [\[CrossRef\]](#) [\[PubMed\]](#)
42. Hansima, M.; Makehelwala, M.; Jinadasa, K.; Wei, Y.; Nanayakkara, K.G.N.; Herath, A.C.; Weerasooriya, R. Fouling of ion exchange membranes used in the electrodialysis reversal advanced water treatment: A review. *Chemosphere* **2021**, *263*, 127951. [\[CrossRef\]](#) [\[PubMed\]](#)
43. Yang, F.; He, Y.; Rosentsvit, L.; Suss, M.E.; Zhang, X.; Gao, T.; Liang, P. Flow-electrode capacitive deionization: A review and new perspectives. *Water Res.* **2021**, *200*, 117222. [\[CrossRef\]](#) [\[PubMed\]](#)
44. Scialdone, O.; D'Angelo, A.; De Lumè, E.; Galia, A. Cathodic reduction of hexavalent chromium coupled with electricity generation achieved by reverse-electrodialysis processes using salinity gradients. *Electrochim. Acta* **2014**, *137*, 258–265. [\[CrossRef\]](#)
45. D'Angelo, A.; Galia, A.; Scialdone, O. Cathodic abatement of Cr(VI) in water by microbial reverse-electrodialysis cells. *J. Electroanal. Chem.* **2015**, *748*, 40–46. [\[CrossRef\]](#)
46. Babilas, D.; Muszyński, J.; Milewski, A.; Leśniak-Ziółkowska, K.; Dydo, P. Electrodialysis enhanced with disodium EDTA as an innovative method for separating Cu(II) ions from zinc salts in wastewater. *Chem. Eng. J.* **2021**, *408*, 127908. [\[CrossRef\]](#)
47. López, J.; Gibert, O.; Cortina, J.L. Integration of membrane technologies to enhance the sustainability in the treatment of metal-containing acidic liquid wastes. An overview. *Sep. Purif. Technol.* **2021**, *265*, 118485. [\[CrossRef\]](#)
48. Wang, C.; Li, T.; Yu, G.; Deng, S. Removal of low concentrations of nickel ions in electroplating wastewater by combination of electrodialysis and electrodeposition. *Chemosphere* **2021**, *263*, 128208. [\[CrossRef\]](#)
49. Alliou, F.-M.; Kapruwan, P.; Milne, N.; Kong, L.; Fattaccioli, J.; Chen, Y.; Dumée, L.F. Electro-capture of heavy metal ions with carbon cloth integrated microfluidic devices. *Sep. Purif. Technol.* **2018**, *194*, 26–32. [\[CrossRef\]](#)
50. Carpanedo de Moraes Nepel, T.; Landers, R.; Gurgel Adeodato Vieira, M.; Florencio de Almeida Neto, A. Metallic copper removal optimization from real wastewater using pulsed electrodeposition. *J. Hazard. Mater.* **2020**, *384*, 121416. [\[CrossRef\]](#)
51. Ning, D.; Yang, C.; Wu, H. Ultrafast Cu²⁺ recovery from waste water by jet electrodeposition. *Sep. Purif. Technol.* **2019**, *220*, 217–221. [\[CrossRef\]](#)
52. Verduzco, L.E.; Oliva, J.; Oliva, A.I.; Macias, E.; Garcia, C.R.; Herrera-Trejo, M.; Pariona, N.; Mtz-Enriquez, A.I. Enhanced removal of arsenic and chromium contaminants from drinking water by electrodeposition technique using graphene composites. *Mater. Chem. Phys.* **2019**, *229*, 197–209. [\[CrossRef\]](#)
53. Li, M.; Zhou, S.; Xu, Y.; Liu, Z.; Ma, F.; Zhi, L.; Zhou, X. Simultaneous Cr(VI) reduction and bioelectricity generation in a dual chamber microbial fuel cell. *Chem. Eng. J.* **2018**, *334*, 1621–1629. [\[CrossRef\]](#)
54. Wang, Y.; Chen, Y.; Wen, Q. Microbial fuel cells: Enhancement with a polyaniline/carbon felt capacitive bioanode and reduction of Cr(VI) using the intermittent operation. *Environ. Chem. Lett.* **2017**, *16*, 319–326. [\[CrossRef\]](#)
55. Zhang, H.; Xu, W.; Wu, Z.; Zhou, M.; Jin, T. Removal of Cr(VI) with Cogeneration of Electricity by an Alkaline Fuel Cell Reactor. *J. Phys. Chem. C* **2013**, *117*, 14479–14484. [\[CrossRef\]](#)
56. Xu, W.; Zhang, H.; Li, G.; Wu, Z. A urine/Cr(VI) fuel cell—Electrical power from processing heavy metal and human urine. *J. Electroanal. Chem.* **2016**, *764*, 38–44. [\[CrossRef\]](#)
57. Hussin, F.; Aroua, M.K.; Szlachta, M. Combined solar electrocoagulation and adsorption processes for Pb(II) removal from aqueous solution. *Chem. Eng. Process.-Process Intensif.* **2019**, *143*, 107619. [\[CrossRef\]](#)
58. Akbal, F.; Camcı, S. Copper, chromium and nickel removal from metal plating wastewater by electrocoagulation. *Desalination* **2011**, *269*, 214–222. [\[CrossRef\]](#)
59. Ghosh, P.; Samanta, A.N.; Ray, S. Reduction of COD and removal of Zn²⁺ from rayon industry wastewater by combined electro-Fenton treatment and chemical precipitation. *Desalination* **2011**, *266*, 213–217. [\[CrossRef\]](#)
60. Al-Shannag, M.; Al-Qodah, Z.; Bani-Melhem, K.; Qtaishat, M.R.; Alkasrawi, M. Heavy metal ions removal from metal plating wastewater using electrocoagulation: Kinetic study and process performance. *Chem. Eng. J.* **2015**, *260*, 749–756. [\[CrossRef\]](#)
61. Gajda, I.; Stinchcombe, A.; Greenman, J.; Melhuish, C.; Ieropoulos, I. Microbial fuel cell—A novel self-powered wastewater electrolyser for electrocoagulation of heavy metals. *Int. J. Hydrogen Energy* **2017**, *42*, 1813–1819. [\[CrossRef\]](#)

62. Tran, T.-K.; Chiu, K.-F.; Lin, C.-Y.; Leu, H.-J. Electrochemical treatment of wastewater: Selectivity of the heavy metals removal process. *Int. J. Hydrogen Energy* **2017**, *42*, 27741–27748. [\[CrossRef\]](#)
63. Mojiri, A.; Ohashi, A.; Ozaki, N.; Kindaichi, T. Pollutants removal from synthetic wastewater by the combined electrochemical, adsorption and sequencing batch reactor (SBR). *Ecotoxicol. Environ. Saf.* **2018**, *161*, 137–144. [\[CrossRef\]](#) [\[PubMed\]](#)
64. Basha, C.A.; Somasundaram, M.; Kannadasan, T.; Lee, C.W. Heavy metals removal from copper smelting effluent using electrochemical filter press cells. *Chem. Eng. J.* **2011**, *171*, 563–571. [\[CrossRef\]](#)
65. Maarof, H.I.; Ajeel, M.A.; Daud, W.M.A.W.; Aroua, M.K. Electrochemical Properties and Electrode Reversibility Studies of Palm Shell Activated Carbon for Heavy Metal Removal. *Electrochim. Acta* **2017**, *249*, 96–103. [\[CrossRef\]](#)
66. Colantonio, N.; Kim, Y. Cadmium (II) removal mechanisms in microbial electrolysis cells. *J. Hazard. Mater.* **2016**, *311*, 134–141. [\[CrossRef\]](#)
67. Eivazihollagh, A.; Bäckström, J.; Norgren, M.; Edlund, H. Electrochemical recovery of copper complexed by DTPA and C12-DTPA from aqueous solution using a membrane cell. *J. Chem. Technol. Biotechnol.* **2018**, *93*, 1421–1431. [\[CrossRef\]](#)
68. Eivazihollagh, A.; Bäckström, J.; Norgren, M.; Edlund, H. Influences of the operational variables on electrochemical treatment of chelated Cu(II) in alkaline solutions using a membrane cell. *J. Chem. Technol. Biotechnol.* **2017**, *92*, 1436–1445. [\[CrossRef\]](#)
69. Farooq, R.; Wang, Y.; Lin, F.; Shaukat, S.F.; Donaldson, J.; Chouhdary, A.J. Effect of ultrasound on the removal of copper from the model solutions for copper electrolysis process. *Water Res.* **2002**, *36*, 3165–3169. [\[CrossRef\]](#)
70. Luo, H.; Liu, G.; Zhang, R.; Bai, Y.; Fu, S.; Hou, Y. Heavy metal recovery combined with H₂ production from artificial acid mine drainage using the microbial electrolysis cell. *J. Hazard. Mater.* **2014**, *270*, 153–159. [\[CrossRef\]](#)
71. Tao, H.C.; Lei, T.; Shi, G.; Sun, X.N.; Wei, X.Y.; Zhang, L.J.; Wu, W.M. Removal of heavy metals from fly ash leachate using combined bioelectrochemical systems and electrolysis. *J. Hazard. Mater.* **2014**, *264*, 1–7. [\[CrossRef\]](#)
72. Baticle, P.; Kiefer, C.; Lakhchaf, N.; Leclerc, O.; Persin, M.; Sarrazin, J. Treatment of nickel containing industrial effluents with a hybrid process comprising of polymer complexation–ultrafiltration–electrolysis. *Sep. Purif. Technol.* **2000**, *18*, 195–207. [\[CrossRef\]](#)
73. Gylie, O.; Aikaite, J.; Nivinskiene, O. Recovery of EDTA from complex solution using Cu(II) as precipitant and Cu(II) subsequent removal by electrolysis. *J. Hazard. Mater.* **2004**, *116*, 119–124. [\[CrossRef\]](#)
74. Nemati, M.; Hosseini, S.M.; Shabanian, M. Novel electrodialysis cation exchange membrane prepared by 2-acrylamido-2-methylpropane sulfonic acid; heavy metal ions removal. *J. Hazard. Mater.* **2017**, *337*, 90–104. [\[CrossRef\]](#)
75. Hunsom, M.; Pruksathorn, K.; Damronglerd, S.; Vergnes, H.; Duverneuil, P. Electrochemical treatment of heavy metals (Cu²⁺, Cr⁶⁺, Ni²⁺) from industrial effluent and modeling of copper reduction. *Water Res.* **2005**, *39*, 610–616. [\[CrossRef\]](#)
76. Martins, R.; Britto-Costa, P.H.; Ruotolo, L.A. Removal of toxic metals from aqueous effluents by electrodeposition in a spouted bed electrochemical reactor. *Environ. Technol.* **2012**, *33*, 1123–1131. [\[CrossRef\]](#)
77. Xing, W.; Liang, J.; Tang, W.; He, D.; Yan, M.; Wang, X.; Luo, Y.; Tang, N.; Huang, M. Versatile applications of capacitive deionization (CDI)-based technologies. *Desalination* **2020**, *482*, 114390. [\[CrossRef\]](#)
78. Weng, J.-z.; Wang, S.-y.; Zhang, P.-x.; Li, C.-p.; Wang, G. A review of metal-organic framework-derived carbon electrode materials for capacitive deionization. *New Carbon Mater.* **2021**, *36*, 117–132. [\[CrossRef\]](#)
79. Tang, K.; Hong, T.Z.X.; You, L.; Zhou, K. Carbon–metal compound composite electrodes for capacitive deionization: Synthesis, development and applications. *J. Mater. Chem. A* **2019**, *7*, 26693–26743. [\[CrossRef\]](#)
80. Porada, S.; Zhao, R.; van der Wal, A.; Presser, V.; Biesheuvel, P.M. Review on the science and technology of water desalination by capacitive deionization. *Prog. Mater. Sci.* **2013**, *58*, 1388–1442. [\[CrossRef\]](#)
81. Zhao, X.; Wei, H.; Zhao, H.; Wang, Y.; Tang, N. Electrode materials for capacitive deionization: A review. *J. Electroanal. Chem.* **2020**, *873*, 114416. [\[CrossRef\]](#)
82. Luciano, M.A.; Ribeiro, H.; Bruch, G.E.; Silva, G.G. Efficiency of capacitive deionization using carbon materials based electrodes for water desalination. *J. Electroanal. Chem.* **2020**, *859*, 113840. [\[CrossRef\]](#)
83. Lellala, K. Sulfur embedded on in-situ carbon nanodisc decorated on graphene sheets for efficient photocatalytic activity and capacitive deionization method for heavy metal removal. *J. Mater. Res. Technol.* **2021**, *13*, 1555–1566. [\[CrossRef\]](#)
84. Salitra, G.; Soffer, A.; Eliad, L.; Cohen, Y.; Aurbach, D. Carbon Electrodes for Double-Layer Capacitors I. Relations Between Ion and Pore Dimensions. *J. Electrochem. Soc.* **2000**, *147*, 2486. [\[CrossRef\]](#)
85. Farmer, J.C.; Bahowick, S.M.; Harrar, J.E.; Fix, D.V.; Martinelli, R.E.; Vu, A.K.; Carroll, K.L. Electrosorption of Chromium Ions on Carbon Aerogel Electrodes as a Means of Remediating Ground Water. *Energy Fuels* **1997**, *11*, 337–347. [\[CrossRef\]](#)
86. Li, Y.; Stewart, T.C.; Tang, H.L. A comparative study on electrosorptive rates of metal ions in capacitive deionization. *J. Water Process Eng.* **2018**, *26*, 257–263. [\[CrossRef\]](#)
87. Wang, C.; Chen, L.; Liu, S. Activated carbon fiber for adsorption/electrodeposition of Cu (II) and the recovery of Cu (0) by controlling the applied voltage during membrane capacitive deionization. *J. Colloid Interface Sci.* **2019**, *548*, 160–169. [\[CrossRef\]](#)
88. Fan, C.S.; Tseng, S.C.; Li, K.C.; Hou, C.H. Electro-removal of arsenic(III) and arsenic(V) from aqueous solutions by capacitive deionization. *J. Hazard. Mater.* **2016**, *312*, 208–215. [\[CrossRef\]](#)
89. Huang, S.Y.; Fan, C.S.; Hou, C.H. Electro-enhanced removal of copper ions from aqueous solutions by capacitive deionization. *J. Hazard. Mater.* **2014**, *278*, 8–15. [\[CrossRef\]](#)
90. Chen, L.; Wang, C.; Liu, S.; Zhu, L. Investigation of adsorption/desorption behavior of Cr(VI) at the presence of inorganic and organic substance in membrane capacitive deionization (MCDI). *J. Environ. Sci. (China)* **2019**, *78*, 303–314. [\[CrossRef\]](#)

91. Liu, X.; Wu, J.; Wang, J. Electro-enhanced removal of cobalt ions from aqueous solution by capacitive deionization. *Sci. Total Environ.* **2019**, *697*, 134144. [CrossRef]
92. Cao, Z.; Zhang, C.; Yang, Z.; Qin, Q.; Zhang, Z.; Wang, X.; Shen, J. Preparation of Carbon Aerogel Electrode for Electrosorption of Copper Ions in Aqueous Solution. *Materials* **2019**, *12*, 1864. [CrossRef]
93. Yang, Z.-Y.; Jin, L.-J.; Lu, G.-Q.; Xiao, Q.-Q.; Zhang, Y.-X.; Jing, L.; Zhang, X.-X.; Yan, Y.-M.; Sun, K.-N. Sponge-Templated Preparation of High Surface Area Graphene with Ultrahigh Capacitive Deionization Performance. *Adv. Funct. Mater.* **2014**, *24*, 3917–3925. [CrossRef]
94. Liu, L.; Guo, X.; Tallon, R.; Huang, X.; Chen, J. Highly porous N-doped graphene nanosheets for rapid removal of heavy metals from water by capacitive deionization. *Chem. Commun. (Camb.)* **2017**, *53*, 881–884. [CrossRef]
95. Yang, X.; Zhu, J.; Qiu, L.; Li, D. Bioinspired effective prevention of restacking in multilayered graphene films: Towards the next generation of high-performance supercapacitors. *Adv. Mater.* **2011**, *23*, 2833–2838. [CrossRef]
96. Sui, Z.; Meng, Q.; Zhang, X.; Ma, R.; Cao, B. Green synthesis of carbon nanotube–graphene hybrid aerogels and their use as versatile agents for water purification. *J. Mater. Chem.* **2012**, *22*, 8767–8771. [CrossRef]
97. Liu, C.; Wu, T.; Hsu, P.C.; Xie, J.; Zhao, J.; Liu, K.; Sun, J.; Xu, J.; Tang, J.; Ye, Z.; et al. Direct/Alternating Current Electrochemical Method for Removing and Recovering Heavy Metal from Water Using Graphene Oxide Electrode. *ACS Nano* **2019**, *13*, 6431–6437. [CrossRef] [PubMed]
98. Peng, J.; Zhong, K.; Huang, W.; Hou, X.; Gao, H.; Fang, Z.; Li, L. Regulation of an Inner Helmholtz Plane by hierarchical porous biomass activated carbon for stable cathode electrolyte interphase films. *Vacuum* **2021**, *191*, 110331. [CrossRef]
99. Biesheuvel, M. Activated carbon is an electron-conducting amphoteric ion adsorbent. *arXiv* **2015**, arXiv:1509.06354.
100. Porada, S.; Weinstein, L.; Dash, R.; van der Wal, A.; Bryjak, M.; Gogotsi, Y.; Biesheuvel, P.M. Water desalination using capacitive deionization with microporous carbon electrodes. *ACS Appl. Mater. Interfaces* **2012**, *4*, 1194–1199. [CrossRef]
101. Porada, S.; Borchardt, L.; Oschatz, M.; Bryjak, M.; Atchison, J.S.; Keesman, K.J.; Kaskel, S.; Biesheuvel, P.M.; Presser, V. Direct prediction of the desalination performance of porous carbon electrodes for capacitive deionization. *Energy Environ. Sci.* **2013**, *6*, 3700–3712. [CrossRef]
102. Legrand, L.; Shu, Q.; Tedesco, M.; Dykstra, J.; Hamelers, H.V.M. Role of ion exchange membranes and capacitive electrodes in membrane capacitive deionization (MCDI) for CO₂ capture. *J. Colloid Interface Sci.* **2019**, *564*, 478–490. [CrossRef] [PubMed]
103. Dai, L.; Xue, Y.; Qu, L.; Choi, H.J.; Baek, J.B. Metal-free catalysts for oxygen reduction reaction. *Chem. Rev.* **2015**, *115*, 4823–4892. [CrossRef] [PubMed]
104. Nistor, R.; Newns, D.; Martyna, G. The Role of Chemistry in Graphene Doping for Carbon-Based Electronics. *ACS Nano* **2011**, *5*, 3096–3103. [CrossRef] [PubMed]
105. Zhao, C.; Zhang, S.; Sun, N.; Zhou, H.; Wang, G.; Zhang, Y.; Zhang, H.; Zhao, H. Converting eggplant biomass into multifunctional porous carbon electrodes for self-powered capacitive deionization. *Environ. Sci. Water Res. Technol.* **2019**, *5*, 1054–1063. [CrossRef]
106. Zhang, X.F.; Wang, B.; Yu, J.; Wu, X.N.; Zang, Y.H.; Gao, H.C.; Su, P.C.; Hao, S.Q. Three-dimensional honeycomb-like porous carbon derived from corncob for the removal of heavy metals from water by capacitive deionization. *RSC Adv.* **2018**, *8*, 1159–1167. [CrossRef]
107. Mamaril, G.S.S.; de Luna, M.D.G.; Bindumadhavan, K.; Ong, D.C.; Pimentel, J.A.I.; Doong, R.-A. Nitrogen and fluorine co-doped 3-dimensional reduced graphene oxide architectures as high-performance electrode material for capacitive deionization of copper ions. *Sep. Purif. Technol.* **2021**, *272*, 117559. [CrossRef]
108. Wang, R.; Xu, B.; Chen, Y.; Yin, X.; Liu, Y.; Yang, W. Electro-enhanced adsorption of lead ions from slightly-polluted water by capacitive deionization. *Sep. Purif. Technol.* **2022**, *282*, 120122. [CrossRef]
109. Ji, Q.; Hu, C.; Liu, H.; Qu, J. Development of nitrogen-doped carbon for selective metal ion capture. *Chem. Eng. J.* **2018**, *350*, 608–615. [CrossRef]
110. Borghei, M.; Laocharoen, N.; Kibena-Pöldsepp, E.; Johansson, L.-S.; Campbell, J.; Kauppinen, E.; Tammeveski, K.; Rojas, O.J. Porous N,P-doped carbon from coconut shells with high electrocatalytic activity for oxygen reduction: Alternative to Pt-C for alkaline fuel cells. *Appl. Catal. B Environ.* **2017**, *204*, 394–402. [CrossRef]
111. Liu, P.; Yan, T.; Zhang, J.; Shi, L.; Zhang, D. Separation and recovery of heavy metal ions and salt ions from wastewater by 3D graphene-based asymmetric electrodes via capacitive deionization. *J. Mater. Chem. A* **2017**, *5*, 14748–14757. [CrossRef]
112. Zhang, Y.-J.; Xue, J.-Q.; Li, F.; Dai, J.I.Z.; Zhang, X.-Z.-Y. Preparation of polypyrrole/chitosan/carbon nanotube composite nano-electrode and application to capacitive deionization process for removing Cu²⁺. *Chem. Eng. Process.-Process Intensif.* **2019**, *139*, 121–129. [CrossRef]
113. Yang, L.; Shi, Z.; Yang, W. Enhanced capacitive deionization of lead ions using air-plasma treated carbon nanotube electrode. *Surf. Coat. Technol.* **2014**, *251*, 122–127. [CrossRef]
114. Gao, Y.; Li, Z.; Fu, Z.; Zhang, H.; Wang, G.; Zhou, H. Highly selective capacitive deionization of copper ions in FeS₂@N, S co-doped carbon electrode from wastewater. *Sep. Purif. Technol.* **2021**, *262*, 118336. [CrossRef]
115. Bharath, G.; Rambabu, K.; Banat, F.; Hai, A.; Arangadi, A.F.; Ponpandian, N. Enhanced electrochemical performances of peanut shell derived activated carbon and its Fe₃O₄ nanocomposites for capacitive deionization of Cr(VI) ions. *Sci. Total Environ.* **2019**, *691*, 713–726. [CrossRef]
116. Wang, H.; He, Y.; Chai, L.; Lei, H.; Yang, W.; Hou, L.; Yuan, T.; Jin, L.; Tang, C.-J.; Luo, J. Highly-dispersed Fe₂O₃@C electrode materials for Pb²⁺ removal by capacitive deionization. *Carbon* **2019**, *153*, 12–20. [CrossRef]

117. Bharath, G.; Alhseinat, E.; Ponpandian, N.; Khan, M.A.; Siddiqui, M.R.; Ahmed, F.; Alsharaeh, E.H. Development of adsorption and electrosorption techniques for removal of organic and inorganic pollutants from wastewater using novel magnetite/porous graphene-based nanocomposites. *Sep. Purif. Technol.* **2017**, *188*, 206–218. [[CrossRef](#)]
118. Li, P.; Gui, Y.; Blackwood, D.J. Development of a Nanostructured alpha-MnO₂/Carbon Paper Composite for Removal of Ni²⁺/Mn²⁺ Ions by Electrosorption. *ACS Appl. Mater. Interfaces* **2018**, *10*, 19615–19625. [[CrossRef](#)]
119. Liu, L.; Qiu, G.; Suib, S.L.; Liu, F.; Zheng, L.; Tan, W.; Qin, L. Enhancement of Zn²⁺ and Ni²⁺ removal performance using a deionization pseudocapacitor with nanostructured birnessite and its carbon nanotube composite electrodes. *Chem. Eng. J.* **2017**, *328*, 464–473. [[CrossRef](#)]
120. Bautista-Patacsil, L.; Lazarte, J.P.L.; Dipasupil, R.C.; Pasco, G.Y.; Eusebio, R.C.; Orbecido, A.; Doong, R. Deionization utilizing reduced graphene oxide-titanium dioxide nanotubes composite for the removal of Pb²⁺ and Cu²⁺. *J. Environ. Chem. Eng.* **2020**, *8*, 103063. [[CrossRef](#)]
121. Li, J.; Wang, X.; Wang, H.; Wang, S.; Hayat, T.; Alsaedi, A.; Wang, X. Functionalization of biomass carbonaceous aerogels and their application as electrode materials for electro-enhanced recovery of metal ions. *Environ. Sci. Nano* **2017**, *4*, 1114–1123. [[CrossRef](#)]
122. Kyaw, H.H.; Myint, M.T.Z.; Al-Harhi, S.; Al-Abri, M. Removal of heavy metal ions by capacitive deionization: Effect of surface modification on ions adsorption. *J. Hazard. Mater.* **2020**, *385*, 121565. [[CrossRef](#)] [[PubMed](#)]
123. Li, S.; Wei, Y.; Kong, Y.; Tao, Y.; Yao, C.; Zhou, R. Electrochemical removal of lead ions using paper electrode of polyaniline/attapulgite composites. *Synth. Met.* **2015**, *199*, 45–50. [[CrossRef](#)]
124. Zhang, Y.; Xue, Q.; Li, F.; Dai, J. Removal of heavy metal ions from wastewater by capacitive deionization using polypyrrole/chitosan composite electrode. *Adsorpt. Sci. Technol.* **2019**, *37*, 205–216. [[CrossRef](#)]
125. Karthik, R.; Meenakshi, S. Synthesis, characterization and Cr(VI) uptake studies of polypyrrole functionalized chitin. *Synth. Met.* **2014**, *198*, 181–187. [[CrossRef](#)]
126. Karthik, R.; Meenakshi, S. Removal of Pb(II) and Cd(II) ions from aqueous solution using polyaniline grafted chitosan. *Chem. Eng. J.* **2015**, *263*, 168–177. [[CrossRef](#)]
127. Hu, C.; Liu, F.; Lan, H.; Liu, H.; Qu, J. Preparation of a manganese dioxide/carbon fiber electrode for electrosorptive removal of copper ions from water. *J. Colloid Interface Sci.* **2015**, *446*, 359–365. [[CrossRef](#)]
128. Jin, W.; Hu, M. High-Performance Capacitive Deionization of Copper Ions at Nanoporous ZnS-Decorated Carbon Felt. *J. Electrochem. Soc.* **2019**, *166*, E29–E34. [[CrossRef](#)]
129. Mohanraj, P.; AllwinEbinesar, J.S.S.; Amala, J.; Bhuvaneshwari, S. Biocomposite based electrode for effective removal of Cr (VI) heavy metal via capacitive deionization. *Chem. Eng. Commun.* **2019**, *207*, 775–789. [[CrossRef](#)]
130. Dong, Q.; Guo, X.; Huang, X.; Liu, L.; Tallon, R.; Taylor, B.; Chen, J. Selective removal of lead ions through capacitive deionization: Role of ion-exchange membrane. *Chem. Eng. J.* **2019**, *361*, 1535–1542. [[CrossRef](#)]
131. Zhao, C.; Zhang, L.; Ge, R.; Zhang, A.; Zhang, C.; Chen, X. Treatment of low-level Cu(II) wastewater and regeneration through a novel capacitive deionization-electrodeionization (CDI-EDI) technology. *Chemosphere* **2019**, *217*, 763–772. [[CrossRef](#)]
132. Hou, S.; Xu, X.; Wang, M.; Lu, T.; Sun, C.Q.; Pan, L. Synergistic conversion and removal of total Cr from aqueous solution by photocatalysis and capacitive deionization. *Chem. Eng. J.* **2018**, *337*, 398–404. [[CrossRef](#)]
133. Huang, Z.; Lu, L.; Cai, Z.; Ren, Z.J. Individual and competitive removal of heavy metals using capacitive deionization. *J. Hazard. Mater.* **2016**, *302*, 323–331. [[CrossRef](#)]
134. Gu, X.; Yang, Y.; Hu, Y.; Hu, M.; Wang, C. Fabrication of Graphene-Based Xerogels for Removal of Heavy Metal Ions and Capacitive Deionization. *ACS Sustain. Chem. Eng.* **2015**, *3*, 1056–1065. [[CrossRef](#)]
135. Pogrebnaya, T.; Jande, Y.A.C.; Alfredo, T. Removal of lead ions from water by capacitive deionization electrode materials derived from chicken feathers. *J. Water Reuse Desalination* **2019**, *9*, 282–291. [[CrossRef](#)]
136. Yang, X.; Liu, L.; Tan, W.; Qiu, G.; Liu, F. High-performance Cu²⁺ adsorption of birnessite using electrochemically controlled redox reactions. *J. Hazard. Mater.* **2018**, *354*, 107–115. [[CrossRef](#)]
137. Li, H.; Zou, L.; Pan, L.; Sun, Z. Using graphene nano-flakes as electrodes to remove ferric ions by capacitive deionization. *Sep. Purif. Technol.* **2010**, *75*, 8–14. [[CrossRef](#)]

Disclaimer/Publisher's Note: The statements, opinions and data contained in all publications are solely those of the individual author(s) and contributor(s) and not of MDPI and/or the editor(s). MDPI and/or the editor(s) disclaim responsibility for any injury to people or property resulting from any ideas, methods, instructions or products referred to in the content.